Integrative Cancer Therapies
2017, Vol. 16(4) 526–539

DOI: 10.1177/1534735416664784
journals.sagepub.com/home/ict
SAGE

# Emodin Exerts an Antiapoptotic Effect on Human Chronic Myelocytic Leukemia K562 Cell Lines by Targeting the PTEN/PI3K-AKT Signaling Pathway and Deleting BCR-ABL

**Chun-Guang Wang, MMed[1], Liang Zhong, MMed[2], Yong-Li Liu, BMed, MMB[1], Xue-Jun Shi, MMed[1], Long-Qin Shi, BN[1], Li Zeng, MMed[1], and Bei-Zhong Liu, MD[1]**

**Abstract**

The BCR-ABL kinase inhibitor, imatinib mesylate, is the front-line treatment for chronic myeloid leukemia, but the emergence of imatinib resistance has led to the search for alternative drug treatments. There is a pressing need, therefore, to develop and test novel drugs. Natural products including plants, microorganisms, and halobios provide rich resources for discovery of anticancer drugs. In this article, we demonstrate that emodin inhibited the growth of K562 cells harboring BCR-ABL in vitro and in vivo, and induced abundant apoptosis, which was correlated with the inhibition of PETN/PI3K/Akt level and deletion of BCR-ABL. These findings suggest that emodin is a promising agent to kill K562 cells harboring BCR-ABL.

**Keywords**

emodin, K562 cells, BCR-ABL, PTEN, PI3K-AKT

Submitted Date: 9 April 2016; Revised Date: 15 July 2016; Acceptance Date: 19 July 2016

## Introduction

Chronic myeloid leukemia (CML) represents a clonal disorder of hematological stem cells containing a constitutively active tyrosine kinase known as BCR-ABL. BCR-ABL confers cells with a survival advantage due to the continuous activation of many downstream signaling pathways including the signal transducer and activator transcription (STAT) and phosphoinositide-3-kinase (PI3K) pathways, rendering cells resistant to apoptosis.

The PI3Ks are a family oflipid kinases that catalyze the phosphorylation of phosphoinositides at the 30-hydroxyl group. A critical product of this reaction is phosphatidylinositol-3,4,5-trisphosphate (PIP3), a vital second messenger, which recruits downstream signaling proteins including AKT and the phosphoinositide-dependent kinase-1 (PDK1).[1]Earlier studies have indicated that the treatment of cells with emodin negatively affects the PI3K/AKT signaling cascade.[2] The PI3K signal transduction pathway has been investigated extensively for its role in oncogenic transformation and in the prevention of apoptosis.[3-5] The fact that AKT overexpression is found in many human cancers, that active AKT promotes resistance to chemo- and radiotherapy, and that AKT activity is sufficient to block apoptosis induced by a number of death stimuli has resulted in intensive studies on the role of AKT as a mediator of the PI3K survival signal. These observations suggest that the inhibition of the PI3K/AKT pathway might be therapeutically important for cancer patients.

Emodin (1,3,8-trihydroxy-6-methylanthraquinone) is a natural anthraquinone derivative isolated from *Rheum palmatum* L. Pharmacological studies have demonstrated that emodin possesses various biological functions, such as antibacterial, anti-inflammatory, and anticancer, and is a potent inhibitor of casein kinase 2. Previous studies have demonstrated that emodin inhibits cell growth in several

[1]Yongchuan Hospital, Chongqing Medical University, Chongqing, People's Republic of China
[2]Chongqing Medical University, Chongqing, People's Republic of China

**Corresponding Author:**
Bei-Zhong Liu, Central Laboratory of Yongchuan Hospital, Chongqing Medical University, Chongqing 402160, People's Republic of China.
Email: 395015952@qq.com

types of tumor cells.[6-10] But no research has been carried out to investigate the effect of emodin on K562 cells.

In this study, we investigated the molecular mechanisms of emodin on K562 leukemia cells in vitro and in vivo. The results demonstrated that emodin can trigger apoptosis through the inhibition of PI3K/AKT level, upregulating the expression of PTEN and deleting BCR-ABL.

## Materials and Methods

### Reagents and Antibodies

Emodin (purity >98%) was purchased from Calbiochem Inc (San Diego, CA) and was dissolved in dimethyl sulfoxide (DMSO; Sigma, Shanghai, China). Antibodies against c-ABL (C-19), PI3K, AKT, and PTEN were from Santa Cruz Biotechnology (Santa Cruz, CA). Mouse monoclonal antibody against actin was from Sigma-Aldrich (St Louis, MO). Anti-mouse immunoglobulin G and anti-rabbit immunoglobulin G horseradish peroxidase-conjugated antibodies were from Pierce Biotechnology (Rockford, IL). Trizol reagent was from Invitrogen (Carlsbad, CA).

### Cell Culture

Chronic myeloid leukemia K562 cells were obtained from the Cell Bank of Shanghai Institute of Biochemistry & Cell Biology, Chinese Academy of Sciences, and grown in RPMI1640 culture medium (Hyclone, Logan, UT) containing 10% fetal bovine serum (FBS; Hyclone), 100 U/mL benzyl penicillin, and 100 U/mL streptomycin in a regular $CO_2$ incubator at 37°C.

### Cell Viability Assay

3-(4,5-Dimethylthiazol-2-yl)-2,5-diphenyltetrazolium bromide (MTT; Sigma) was used to determine cell survival in a quantitative colorimetric assay. Cells were plated in 96-well tissue culture plates and allowed to attach for 24 hours. Cells were then incubated with fresh medium containing 25, 50, or 100 μmol/L of emodin for 24, 48, and 72 hours, respectively. Twenty microliters of MTT (5 mg/mL) was added to the culture medium 4 hours before harvesting. The medium was then aspirated carefully without disturbing the blue formazan crystals. Then 150 μL DMSO was added to each well to dissolve the formazan crystals while slightly agitating the cells on an automated shaker. The absorbance of the suspension was measured spectrophotometrically at 490 nm by a Benchmark microtiter plate reader (Bio-Rad Laboratories, Hercules, CA). The results were expressed as a percentage of the absorbance present in treated cells compared to control cells. Cell growth inhibition rate (%) was calculated using the following equation: survival ratio (%) = $(1 - A_{\text{treatment}}/A_{\text{control}}) \times 100\%$.

### Assessment of Cell Morphological Changes

To detect morphological evidence of apoptosis, K562 cells were seeded in 50-mL culture bottles ($5 \times 10^5$ cells/bottle) and then incubated with fresh medium containing 50 μmol/L of emodin for 48 hours. Morphology of K562 cells was first observed under light microscope (DIAPHOT300, Nikon, Tokyo, Japan). The K562 cells were then collected, fixed with 4% glutaraldehyde, dehydrated, and embedded with epoxy resin. Ultra-thin sections of 60 nm were prepared for electron microscopy. The ultrastructure of K562 cells was observed under transmission electron microscope (JEM2000, JEOL, Tokyo, Japan) at 100 kV.

### Cell Cycle Analysis

K562 cells ($1 \times 10^5$ cells/mL) were seeded in 6-well plates and cultured with 0.1% DMSO or emodin (25, 50, 100 μmol/L) for 48 hours. Cells treated were harvested, washed with phosphate-buffered saline (PBS), and fixed with 66% ethanol overnight. Cells were centrifuged and washed with PBS, then stained with 50 mg/mL propidium iodide (PI) and 2.5 mg/mL RNase in PBS solution for 30 minutes at room temperature. DNA content was analyzed by flow cytometry at the emission wavelength of 488 nm.

### Apoptotic Cell Determination by Annexin V/PI Staining Assay

Cells were treated with drugs (25, 50, 100 μmol/L emodin) for 48 hours and apoptotic rates were assessed with flow cytometry using Annexin V-fluorescein isothiocyanate (Annexin V-FITC)/PI kit (BD Pharmingen, San Diego, CA). Samples were prepared according to the manufacturer's instruction and analyzed by flow cytometry on FACS Calibur (Becton Dickson, San Diego, CA).

### Apoptotic Cell Determination by DNA Fragmentation Assay

K562 cells ($5\times10^4$ cells) treated with the 25, 50, 100 μmol/L emodin for 48 hours were suspended in 100 μL of 10 mM Tris-HCl and 10 mM ethylenediaminetetraacetic acid (EDTA; pH 8.0). The cells were then treated with 100 mL of a solution that contained 10 mM Tris-HCl, 10 mM EDTA (pH 8.0), 2% sodium dodecyl sulfate (SDS), and 20 mg/mL proteinase K. The mixture was then incubated at 37°C followed by DNA extraction with phenol/chloroform. DNA fragmentation analysis was done with 10 mg DNA prepared from control cells, and cells were treatedwith 25, 50, 100 μmol/L emodin for 48 hours.DNA laddering was analyzed using 2% agarose gel electrophoresis and ethidium bromide staining.

### Reverse Transcriptase-Polymerase Chain Reaction (RT-PCR)

Expression of the BCR-ABL, PI3K, AKT, and PTEN was monitored by RT-PCR. K562 cells ($5\times10^4$ cells) were treated with 25, 50, and 100 μmol/L emodin for 48 hours. After treatment, cells were lysed with 1 mL of RNAse-clean Trizol reagent (Invitrogen, Carlsbad, CA) and then the samples were processed according to the manufacturer's protocol to obtain total cellular RNA. Total cDNAs were synthesized by ThermoScript RT-PCRsystem (Invitrogen Life Technologies, Inc, Carlsbad, CA) and 0.2 μg of total RNA was primed with random hexamers. cDNA amplification was performed as follows: initial denaturation at 94°C for 4 minutes; followed by denaturation at 94°C for 1 minute, annealing at 55°C for 50 seconds, extension at 72°C for 90 seconds for 30 cycles, followed by a final extension at 72°C for 5 minutes. For β-actin amplification, there were a total of 20 PCR cycles. The PCR products were electrophoresed on 2% agarose gel and visualized by staining with ethidium bromide. The sequences for BCR-ABL sense and antisense primers were 5′-TG GTG GGC CTC TCA GTG TCT TA-3′and 5′-TCG GTA GCG CAG GCA GTA GTT C-3′. The sequences for PI3K sense and antisense primers were 5′-A TGC TTC CTG GGG ATA AT-3′and 5′-TCA AAG GCA CGG ATA ACT-3′. The sequences for AKT sense and antisense primers were 5′-CCC ATC ATT GCA ATA GCA GG-3′and 5′-GTT CAA ACT TCT GCT CCT GA-3′; β-actin was used as an internal control. The sequences for β-actin sense and antisense primers were 5′-TGG GGA AGG TGA AGG TCG G-3′and 5′-CTG GAA GAT GG TGA TGG GA-3′.

### Protein Preparation and Western Blot Analysis

K562 cells were treated without or with indicated concentration of emodin for 48 hours. After treatment, the cells were harvested for total protein extraction. Protein concentration was then determined using the Bradford method. For Western blot analysis, equal amounts of protein were loaded and separated by SDS-PAGE. The gels were equilibrated in transfer buffer (50 mM Tris, 40 mM glycine, 0.375% SDS, and 20% methanol) and electrophoretically transferred to a PVDF membrane (Millipore). The membrane was blocked with 5% skim milk in TBST buffer (20 mM Tris-HCl, pH 7.4, 150 mM NaCl, and 0.1% Tween 20) and incubated overnight at 4°C with specific primary antibodies at 1:500 dilution (antibodies against c-ABL [C-19], PI3K, AKT, and PTEN). After washing with TBST, the membrane was incubated with horseradish peroxidase–conjugated secondary antibodies at 1:1000 dilutions for 1 hour. The proteins were then visualized using an enhanced chemiluminescence detection kit (ECL kit, GE Healthcare).

### Nude Mouse Xenograft Model

BALB/c nude mice were bred at the animal facility of Chong Qing Medical University. The mice were housed in barrier facilities with a 12-hour light-dark cycle, with food and water available ad libitum. Transplantable tumors (induced by K562 cells subcutaneous inoculation of a mixture of $2 \times 10^7$ actively growing K562 cells in 100 μL PBS and 100 μL of matrigel to the dorsal side of each nude mouse) were chopped into fragments (about 1.5 $mm^3$), each of which was transplanted into the right or left axillary fossa of 25 nude mice. Palpable tumors of volume 100 to 200 $mm^3$ were developed after 12 days and the mice were randomly divided into 5 groups (with 5 mice per group): negative control group; emodin 25, 50, 100 mg/kg groups and HU120mg/kggroup. The negative control group received 0.9% normal saline containing 1% DMSO. All of these drugs were injected intraperitoneally every day up to 12 days. Tumor size was measured once every 2 days in 2 perpendiculars, and tumor volume (TV) was calculated using the formula: $(ab^2)/2$, where $a$ and $b$ refer to the longer and shorter dimensions, respectively. The body weight of the animals was measured 3 times a week at the same time as the tumor dimension measurement and the mortality was monitored daily. The tumor growth inhibition rate was calculated using the following formula: inhibition rate (%) = (mean tumor weight of negative control group − mean tumor weight of treatment group)/mean tumor weight of negative control group. This experiment was conducted in accordance with the guideline issued by the State Food and Drug Administration (SFDA of China). The animals were housed and cared in accordance with the guidelines established by the National Science Council of Republic China.

### Histopathological Analysis

Tumor tissue was fixed in 10% buffered formalin, paraffin embedded, cut into 4-μm sections that were placed on glass slides, stained with hematoxylin/eosin, and these sections were reviewed under optical microscope.

### Transmission Electron Microscopy (TEM) Analysis of K562 Cell Apoptosis In Vivo

TEM studies were performed as described earlier.[11] In brief, small pieces of tumor tissue (1 $mm^3$) from control and treated mice were fixed with 4% paraformaldehyde and 2% glutaraldehyde in 0.1 M sodium phosphate buffer (pH 7.4) for 4 hours at room temperature (24°C). This was followed by washing the tissue pieces in 0.1 M sodium phosphate buffer (pH 7.4) and then placing them in 2% osmium tetroxide in 0.1 M sodium phosphate buffer (pH 7.4) for 2 hours at room temperature. Dehydration was done in an ascending grade of ethanol, followed by embedding in Epon 812 and polymerization at 60°C for 48 hours. Ultrathin sections (50-70 nm) were obtained

using an Ultracut Ultra microtome (Leica Microsystems GmbH, Wetzlar, Germany) and picked up onto 200-mesh copper grids. The sections were double stained with uranyl acetate and lead citrate, and then analyzed under an FEI Tecnai-12 twin transmission electron microscope equipped with an SIS Mega View II CCD camera at 80 kV (FEI Co, Hillsboro, OR).

### *Western Blot Analysis In Vivo*

A total of 100 to 150 mg tumor specimens were washed in PBS and minced into small pieces using bistouries. Tissue samples were suspended in 1 mL of cold homogenizing buffer and homogenized in an ice-cold grinder. Then the homogenate was centrifuged at 12 000 ×*g*for 15 minutes at 4°C. The concentration of total proteins was measured using a BCA protein assay kit (Pierce, Rockford, IL).The next steps are in line with the aforementioned.

### *RT-PCR Analysis In Vivo*

A total of 100 mg tumor specimens from every treated group was homogenated. Total RNA was isolated from homogenate using Trizol reagent (Invitrogen, Carlsbad, CA). The next steps are in line with the aforementioned.

### *Statistical Analysis*

In vitro, all experiments were performed at least 3 times, and results are expressed as mean ± standard error (SE), unless otherwise stated. GraphPad Prism 4.0 software (GraphPad Software, San Diego, CA) was used for statistical analysis. Comparisons between 2 groups involved 2-sided Student's *t*test, and comparisons among multiple groups involved 1-way ANOVA with post hoc intergroup comparison using Tukey test. $P < .05$ was considered statistically significant.

## Results

### *Emodin Inhibits K562 Cell Viability In Vitro*

To investigate the inhibitory effect of emodin on K562 cells, MTT assay was used to quantify the effect of emodin on K562 cell growth. Through pre-experiment, we determined the time interval in the MTT experiment (data not shown). As shown in Figure 1A and B, emodin caused a decrease of cell viability in K562 cells in a dose- and time-dependent manner when compared with the control. DMSO alone showed no effect on viability of K562 cells.

### *Emodin Induces K562 Cell Division Cycle Arrest at $G_0/G_1$ Phase In Vitro*

The inhibition by emodin of cell growth was further investigated with flow cytometric analysis of cellular

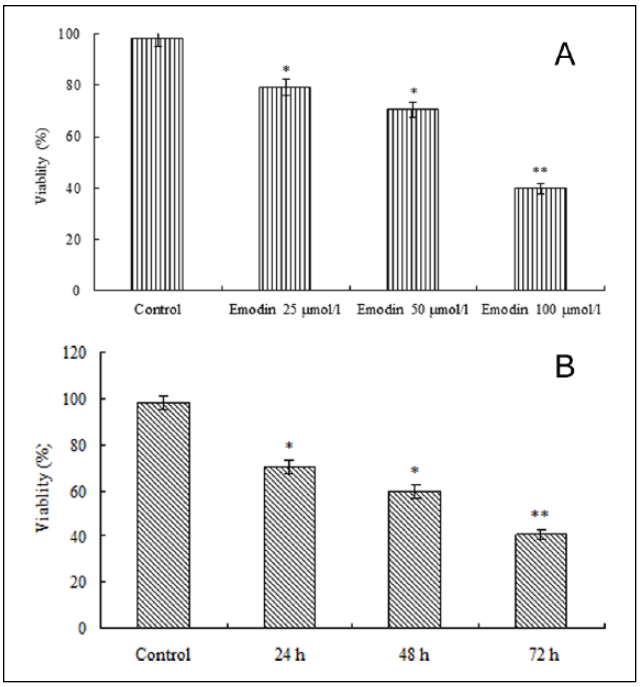


**Figure 1.** Effect of emodin on cell viability in K562 cells. (A) K562 cells were treated without or with emodin (25, 50, and 100 μmol/L for 24 hours). (B) K562 cells were treated without or with 50 μmol/L emodin for 24, 48, and 72 hours. Cell viability was evaluated with MTT assay as described in the Materials and Methods section. All results were expressed as mean ± SEM of 3 independent experiments (n = 3). *$P < .05$ and **$P < .01$ compared withcontrol.

DNA content. As shown in Figure 2A and B, the number of cells in the $G_1$ phase was increased after treatment with 25, 50, and 100 μmol/L of emodin for 24 hours. The percentage of cells in the $G_1$ phase was 57.2% in control, whereas it was increased to 66% to 82% after treatment with 25, 50, and 100 μmol/L of emodin for 24 hours. We also observed that the cells in the S phase decreased while the concentration of emodin increased. More important, we noted a significant decrease of cells in the S phase after treated with 50 μmol/L of emodin. As shown in Figure 2B, emodin resulted in a dose-dependent inhibition of cell cycle. These results suggested that emodin had a prominent ability to inhibit the cell cycle and cause cell cycle arrest at the $G_0/G_1$ phase.

### *Emodin Causes K562 Cell Morphological Changes In Vitro*

Under control conditions, the untreated K562 cells grew well and the skeletons were clear. The cells appeared in a normal circular shape and the nucleoli were evident when observed under optic microscope (Figure 3A) and electron microscope (Figure 3C). After treatment with 40 μmol/L of emodin for 48

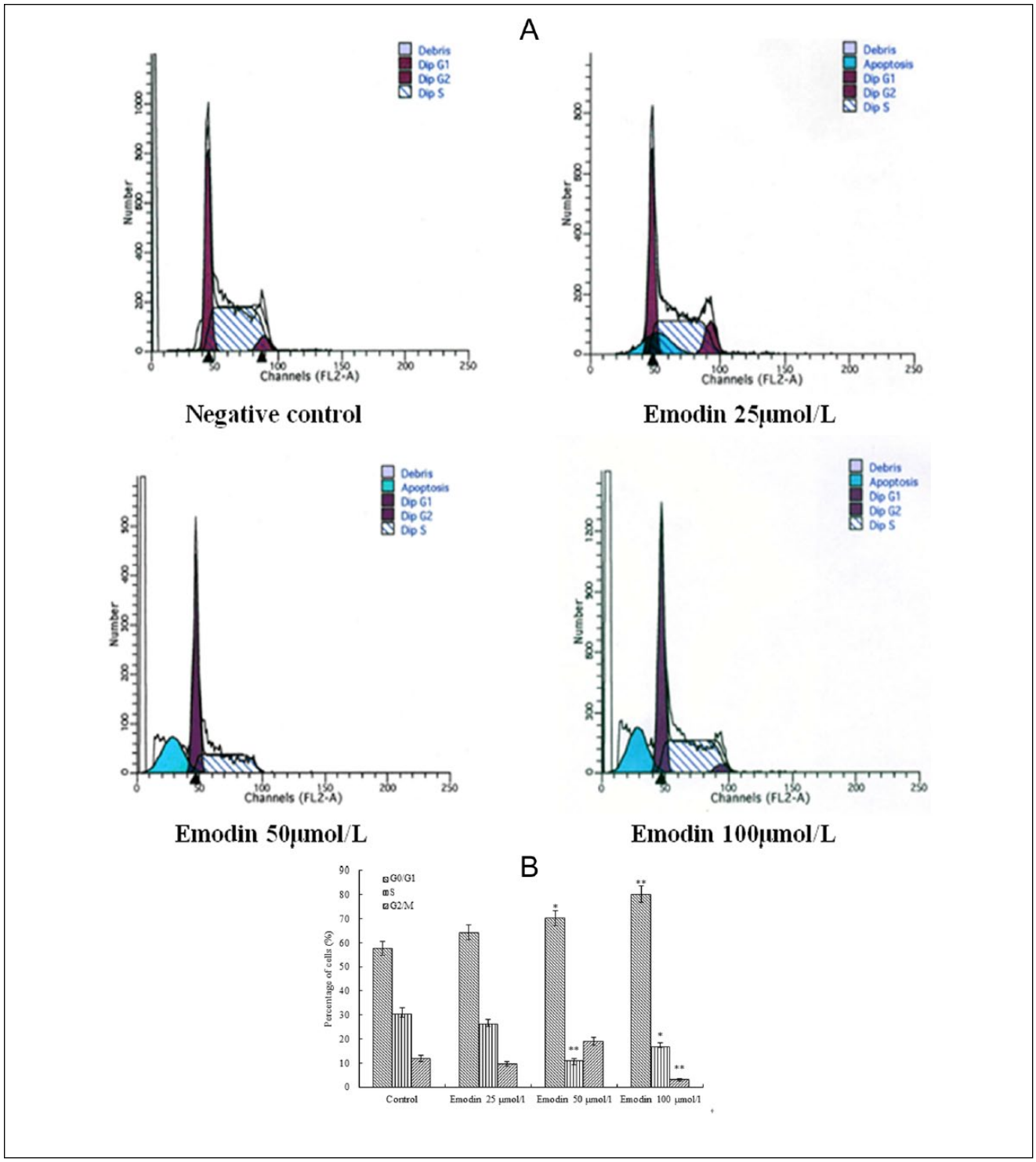


**Figure 2.** Cell cycle distributions of emodin-treated K562 cells were analyzed by flow cytometry. The cells were treated with 0.1% DMSO (negative control group), 25, 50, and 100 μmol/L emodin for 48 hours. (A) Representative data of flow cytometry assay. (B) All results were expressed as mean ± SEM of 3 independent experiments (n = 3). *$P < .05$ and **$P < .01$ compared withcontrol.

hours, the cell volume reduced, cells shrank, nuclear pyknosis was observed, a decreased cell density was noticed, and the apoptotic body appeared (Figure 3B). In addition, morphological characteristics of apoptosis including cellular shrinkage, chromatin margination, condensation, and vacuolization were observed under electron microscope (Figure 3D).

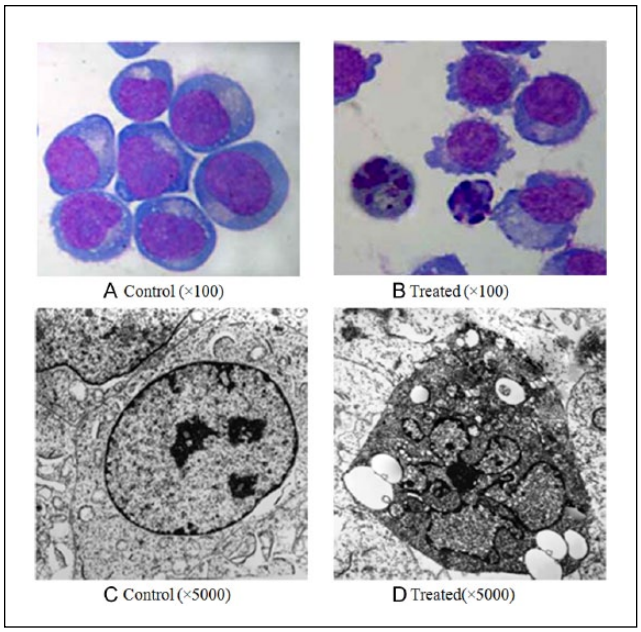


**Figure 3.** Morphological changes induced by emodin in K562 cells. K562 cells were seeded in culture bottles and treated without (A and C) or with 50 μmol/L emodin (B and D) for 48 hours. Apoptotic cells (in B) were characterized by cellular shrinkage (light microscope, 100×). Under a transmission electron microscope, the apoptotic cell (in D) was characterized by marked condensation and margination of chromatin (5000×).

## *Emodin Induces K562 Cell Apoptosis In Vitro*

The deregulation of cell cycle has been reported to correlate with the induction of apoptosis. Based on the appearance of the sub-$G_1$ peak in cell cycle analysis, we further characterized the emodin-induced apoptosis by Annexin V/PI dual staining. This assay divided apoptotic cells into 2 stages: early (Annexin V+/PI−) and late apoptotic/necrotic (Annexin V+/PI+). As shown in Figure 4A, Annexin V/PI double-parameter method is a sensitive detection method for apoptosis. The cells stained mainly by Annexin V-FITC were regarded as the early apoptotic cells. Early apoptosis occurred in K562 cells treated with 25, 50, and 100 μmol/L emodin for 12 hours, and a concentration gradient was shown. The apoptosis rates of treated groups were 8.89%, 22.95%, and 36.06%, respectively; the control group was 2.09% (Figure 4B). There were statistically significant differences between the treated groups and the control group ($P < .001$). In an attempt to further clarify the mechanisms underlying the inhibitory action of emodin on leukemia cells, its effect in the induction of apoptosis on human chronic myelocytic leukemia K562 cells was determined by DNA fragmentation analysis. Emodin-induced apoptosis was found at all tested dosages with 48 hours of incubation. The characteristic apoptotic DNA ladders with multiple bands were observed in these drug-treated groups, while no such DNA ladders were detectable in the negative controls

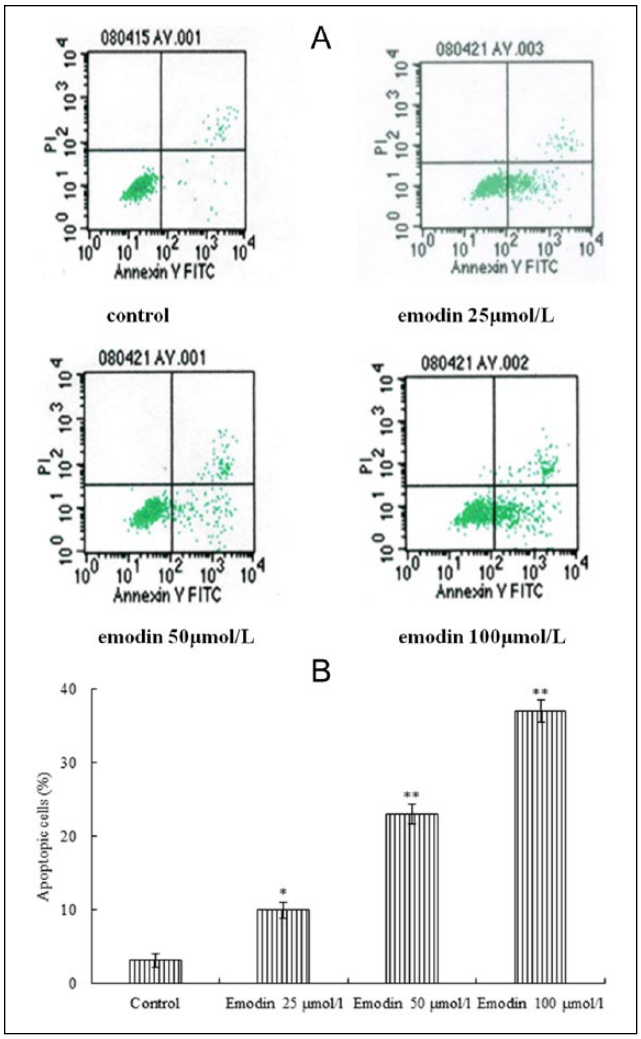


**Figure 4.** The apoptotic rates of K562 cells induced by emodin. K562 cells were treated with 25, 50, and 100 μmol/L emodin for 24 hours. (A) Then cells were collected and stained with FITC-Annexin V to detect cell death phenomena by flow cytometry. *Y* axis shows PI-labeled population, and *X*-axis shows FITC-labeled Annexin-V positive cells. (B) The apoptotic rates of K562 cells induced by emodin. (*$P < .05$, **$P < .01$ vs control). All results were expressed as mean ± SEM of 3 independent experiments (n = 3). *$P < .05$ and **$P < .01$ compared withcontrol.

(Figure 5). With increased concentrations of emodin, multiple bands became more and more clear, which indicated that apoptosis occurred in a dose-dependent manner. Our results indicated that emodin inhibited the growth of K562cells, at least in part, by induction of apoptosis.

## *Emodin Inhibits Tumor Growth in Nude Mice*

The results showed that after 12 days of treatment with emodin, no significant variation in body weight was detected (data not shown), suggesting that emodin did not produce significant nontumor toxicity in tumor-bearing

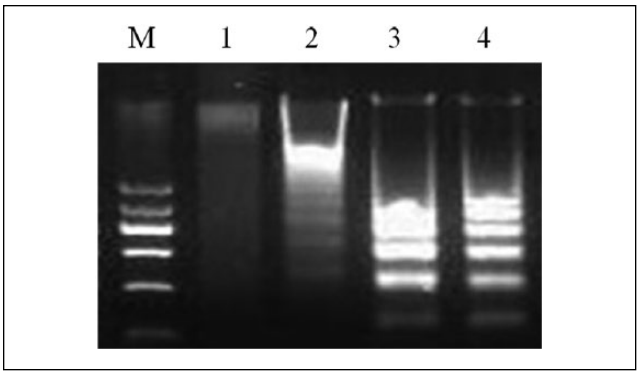


**Figure 5.** The effect of emodin on the induction of apoptosis in K562 cells was determined using DNA fragmentation analysis. DNA was isolated from the cells and analyzed using 2% agarose gel electrophoresis with 1 × TBE buffer and ethidium bromide staining. The apoptotic characteristic laddering pattern of DNA fragments with multiple bands indicated the induction of apoptosis in emodin-treated cells at various conditions but not in the untreated control. Lane M: DNA ladder marker; Lane 1: 48 hours at 0 μmol/L (negative control); Lane 2: 48 hours at 25 μmol/L; Lane 3: 48 hours at 50 μmol/L; Lane 4: 48 hours at 100 μmol/L.

mice. But in the hydroxyurea treatment group, the weight of nude mice (data not shown) was significantly lower than in the negative control group, accompanied by the formation of cachexia. However, the average weight of tumors (Figure 6C) treated with emodin at 25, 50, and 100 mg/kg and HU were 1.02 g, 0.64 g, 0.41 g, and 0.36 g, respectively, versus 1.66 g of negative control tumors, which corresponds to 61.4%, 38.5%, 24.7%, and 21.7% of inhibition ($P < .01$). In addition, the tumor volume of tumors treated with emodin and HU also significantly decreased when compared with the nontreated group (Figure 6A and B). These results suggest that emodin was able to effectively inhibit tumor growth in vivo, and no obvious side effects were found.

## *Effect of Emodin on Transplanted Tumor Histology*

The histopathological changes were observed under optical microscope. The result showed that a large area of necrosis located in periphery of tumors was observed in emodin-treated mice but not in normal saline-treated mice. In normal saline-treated mice, tumors with normal demarcation revealed complete cell shapes with clear cytoplasm and typical nuclei. In contrast, the cell shape was completely destroyed in necrotic tumor tissue derived from emodin-treated mice (Figure 7). In the negative control group (Figure 7A), tumor cells with normal demarcation revealed complete cell shape with clear cytoplasm and typical nuclei. Tumor cells with karyomegaly and anacheromasis were observed. Abnormal division of the nucleus and abundant vessels could also be found. The tumor cell growth was active. There was a small amount of necrotic tissue in the central block of tumor. In the low-dose group (Figure 7B), some cell shape was destroyed in necrotic tumor tissue, and mitotic tumor cells could be found. There were significantly more hemorrhage and necrosis than in the control group. A larger number of tumor cells were apoptotic. In the medium dose group (Figure 7C), several macrophages were approaching to and phagocytosing tumor cells, mitotic figures were seen, and necrosis and hemorrhage were found more easily than in the low-dose group (Figure 7B). In the high-dose group (Figure 7D), the tumor cells with abnormal nuclear division decreased; there were some apoptosis and necrosis and fewer vessels. A large area of necrosis was observed easily. Obvious lymphocytic infiltration, deeply stained cells, and pyknosis were all observed. In the positive control group (Figure 7E), tumor load decreased; some tumor cells necrosed and part of these cells were replaced by connective tissue.

## *Emodin Induces K562 Cell Apoptosis In Vivo*

The morphological features of apoptoticK562 cells in vivo were observed by transmission electron microscopy. Negative control group (Figure 8A): the normal tumor cells with abundant euchromatin had large nuclei, and chromatin margination in the clumped K562 cells was little or none. TEM studies clearly showed intact mitochondria with the double membrane clearly visible, cristae structurally intact, and intramitochondrial matrix consisting of electron-dense granules. All this indicated rapid cell proliferation. Positive control hydroxyurea group (Figure 8E): the main changes of most cells are cellular necrosis, swelling, and heterochromatin margination. The cells with irregular membrane were lumping with apoptotic bodies. Macrophages were beginning to phagocytose tumor cells. Cell microvilli were reduced or absent; mitochondria and other organelle structure were unclear; some nuclei were pyknotic or dissolved. Electron-dense granules ranging from large to small in size could be seen in some cytoplasm, indicating that cell necrosis was serious. In the low concentration emodin treatment group (Figure 8B), many karyopycnotic cells and a few with lumping chromatin were found. Chromatin margination and apoptotic cells were observed. The macrophage spine enclosed tumor cells. In the middle concentration emodin treatment group (Figure 8C), cytoplasm condensation and primary apoptosis were observed. Chromatin margination and the apoptotic cell became more common, and the mitochondrial double membrane was absent. The macrophage spine was enclosing the apoptotic body and was beginning to enclose the tumor cells. In high-concentration emodin treatment group (Figure 8D), the cell membrane was destroyed, and obvious karyopycnosis and margination were observed. Apoptotic bodies formed, and macrophages began to phagocytose the tumor cells. The expansion of

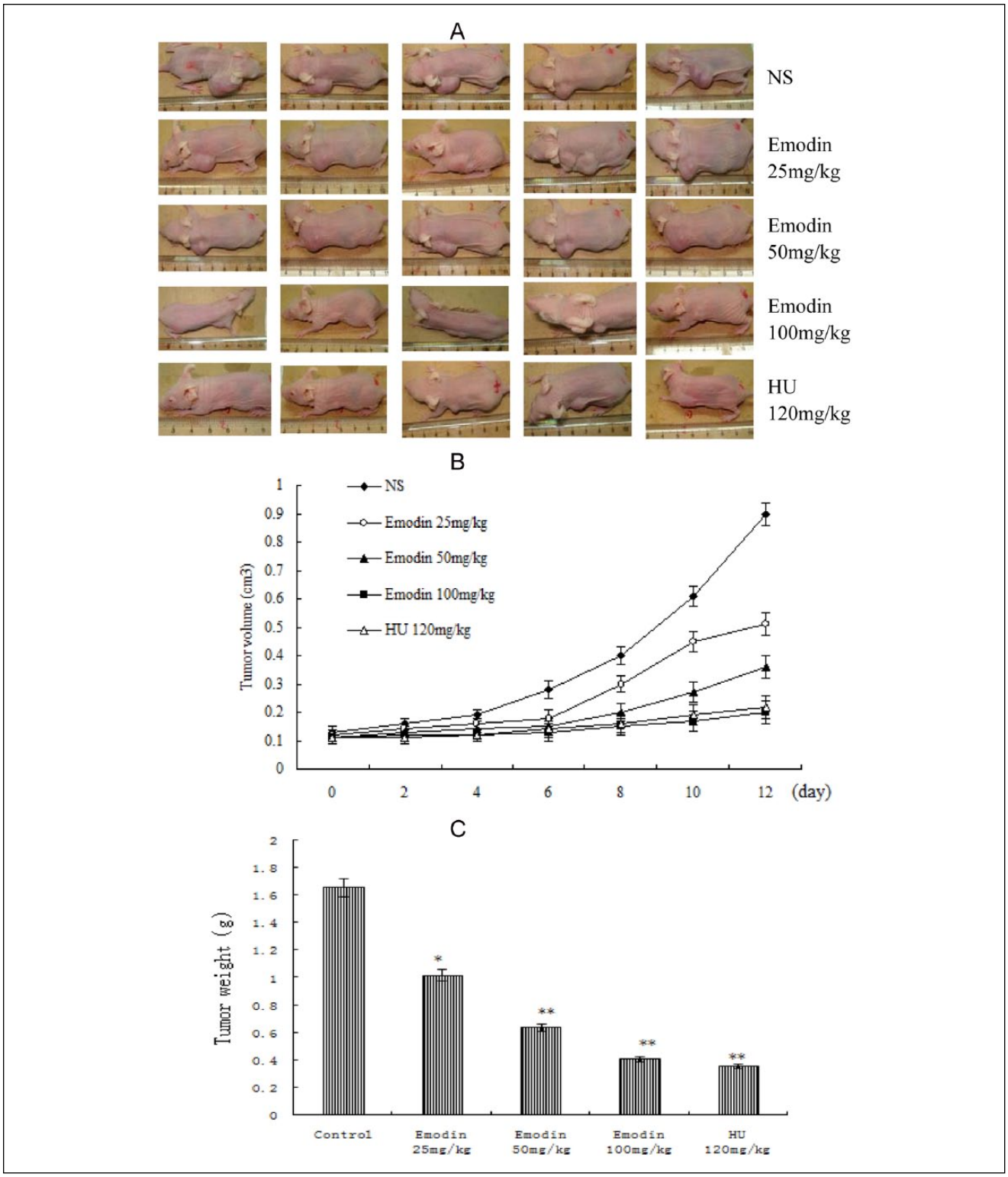


**Figure 6.** The in vivoantitumor effect of emodin on athymic nude mice bearing K562 cells subcutaneously was studied. (A) The tumor size of xenografted tumor in nude mice with K562 cells in each group (control, emodin, and HU treatment groups). (B) Tumor volume of control, emodin, and HU treatment groups. Tumor volume was measured once every 2 days. (C) The weight of tumor of control, emodin, and HU treatment groups. After nude mice were treated for 12 days, the tumors were isolated and weighed. All results were expressed as mean ± SEM. **P* < .05 and ***P* < .01 compared withcontrol.

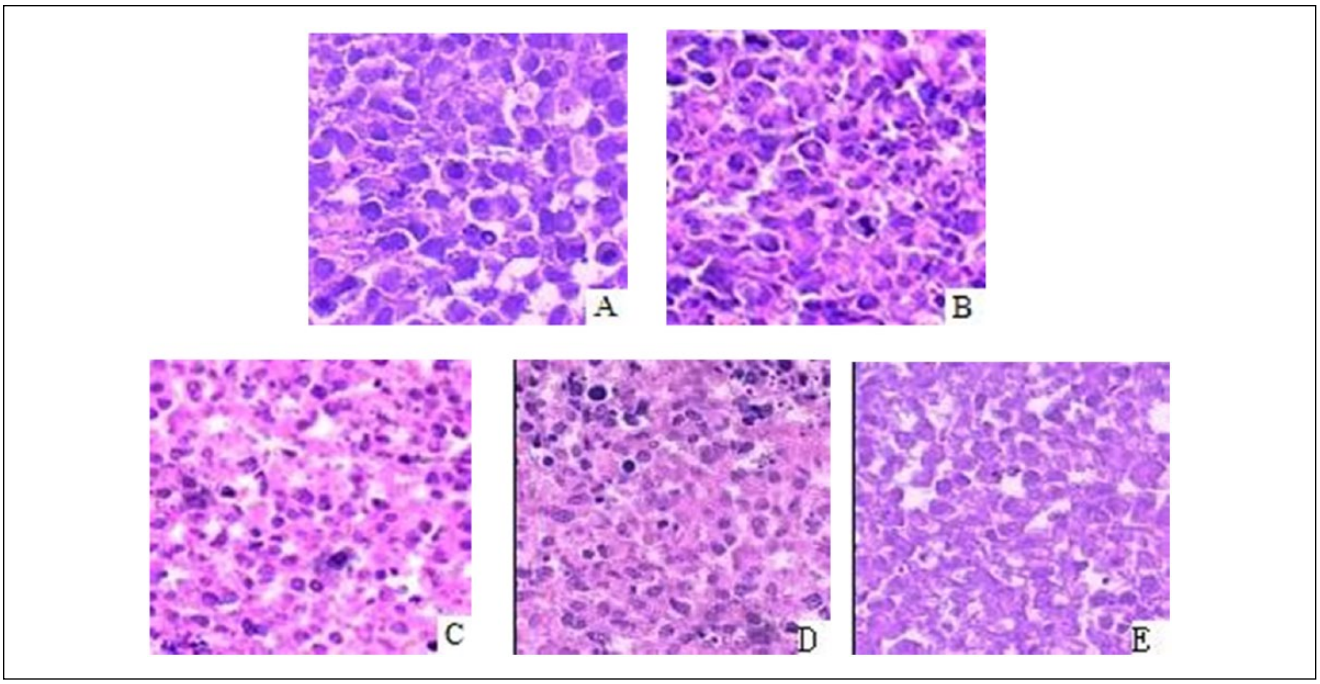


**Figure 7.** Emodin-induced histological changes of tumor mass in mice. BALB/c mice with established K562 cell tumors were injected with the indicated concentration emodin or HU one time every day and sacrificed for removing tumors. Tumor tissue was histological evaluated by hematoxylin-eosin staining. (A) negative control group; (B) emodin 25 mg/kg; (C) emodin 50 mg/kg; (D) emodin 100 mg/kg; (E) HU group. Sections were photographed under 200-fold (down) microscopy.

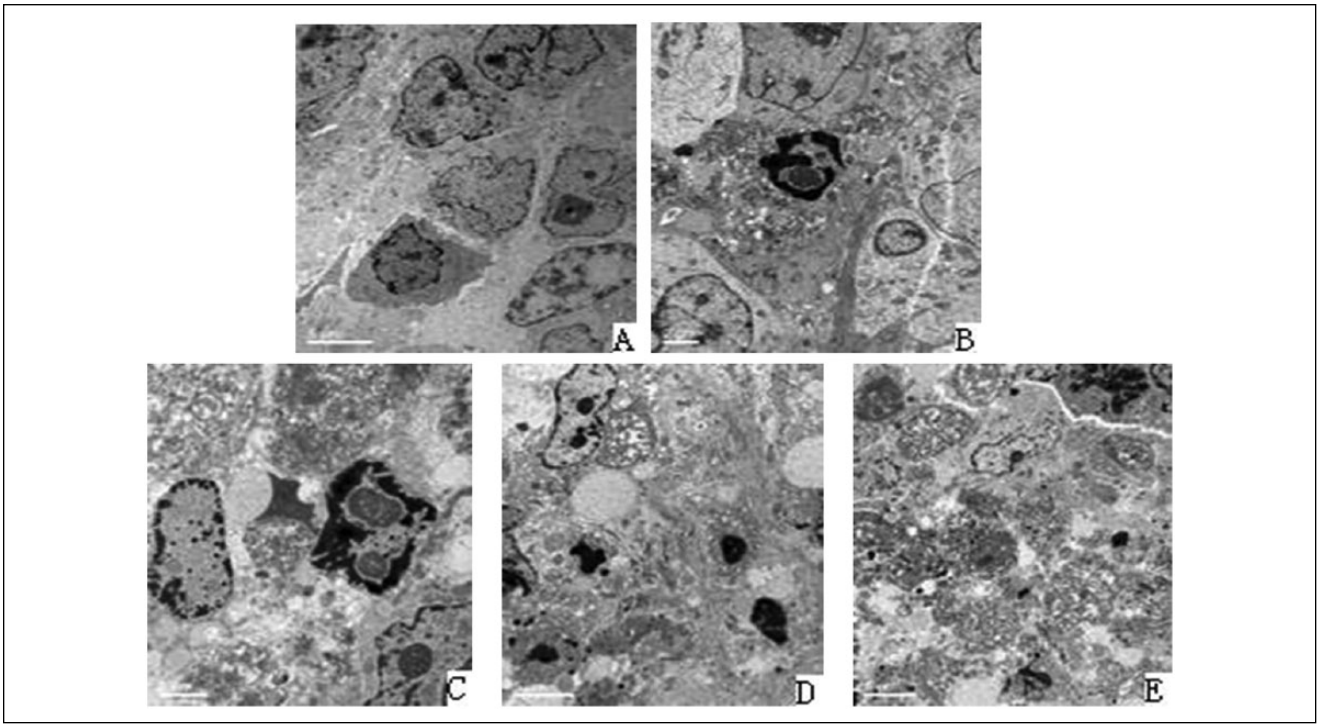


**Figure 8.** Emodin-induced histological changes of tumor mass in mice. BALB/c mice with established K562 cell tumors were injected with the indicated concentration emodin or HU one time every day. Tumor tissue was histologically evaluated by electron microscope. Sections were photographed under indicated-fold transmission electron microscope. (A) Negative control group (×3500); (B) emodin 25 mg/kg (×5000); (C) emodin 50 mg/kg (×5000); (D) emodin 100 mg/kg (×5000); (E) HU 120 mg/kg (×5000).

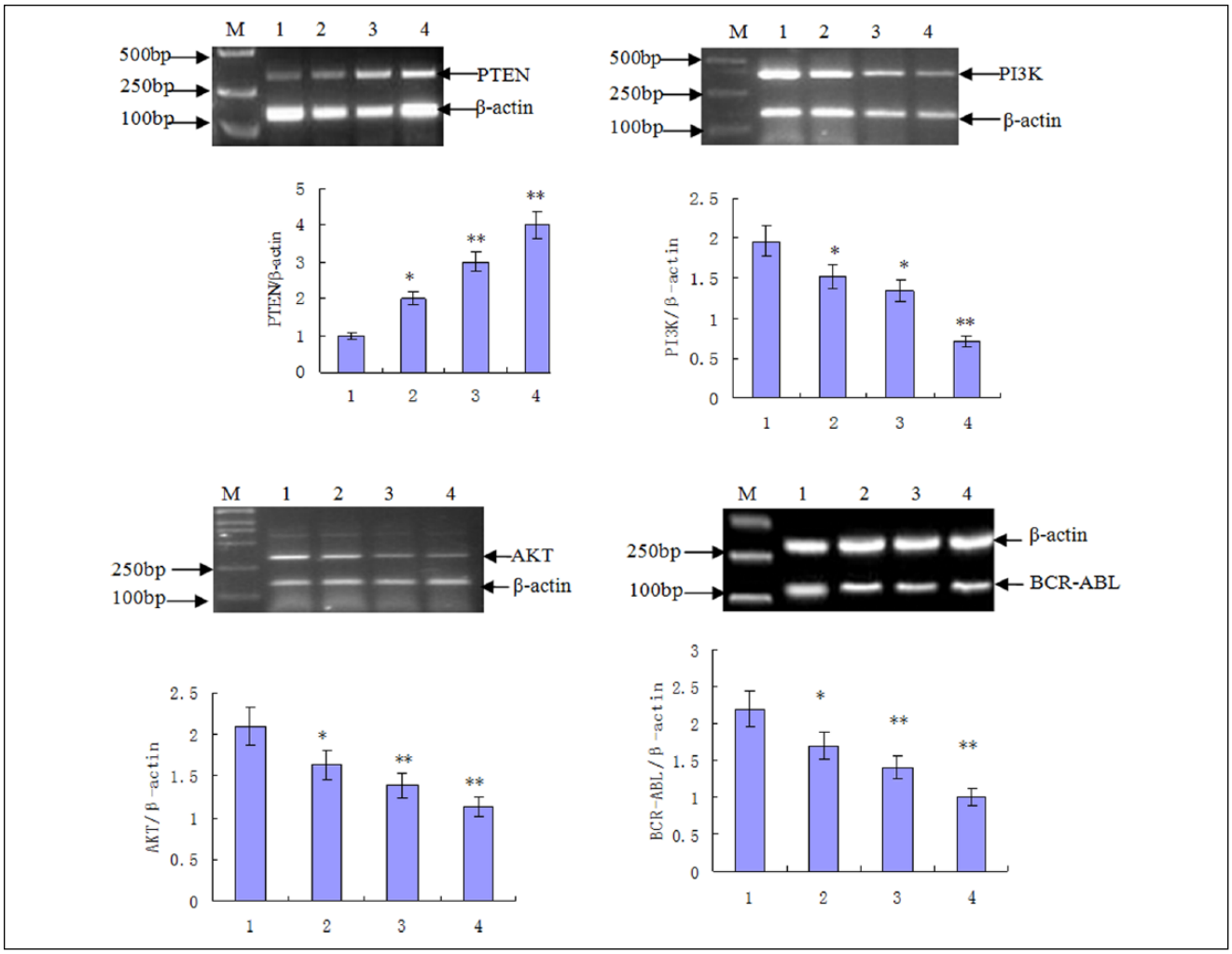


**Figure 9.** The mRNA expressions of PTEN, PI3K, AKT, and BCR-ABL in K562 cell from the emodin-treated group. RT-PCR analysis of the mRNA of PTEN, PI3K, AKT, and BCR-ABL obtained from K562 cell with the emodin or HU. M: DNA marker; 1: negative control; 2: 25 μmol/L group; 3: 50 μmol/L group; 4: 100 μmol/L group. All RT-PCRs were representative of 3 independent experiments (n = 3).

endoplasmic reticulum and some electron-dense granules in cytoplasm were observed easily. In conclusion, emodin could result in the apoptosis of K562 cells in a dose-dependent manner in vivo.

## *Emodin Decreased the BCR-ABL Level*

To address the mechanism of the emodin-mediated growth inhibition in CML cells, we analyzed the expression of BCR-ABL in CML cells treated with or without emodin by RT-PCR and Western blotting. Our study showed emodin dose-dependently decreased BCR-ABL level in vitro and in vivo (Figures 9-11).

## *Emodin Inhibits PI3K/AKT Level*

Emodin inhibited the PI3K/AKT level, which correlated with the enhancement of emodin-induced apoptosis. AKT has been described as a downstream effector of PI3K in a number of models that involve activation of PI3K in survival signaling. We investigated whether AKT could be inactivated in K562 cells in response to emodin. To demonstrate that emodin induced apoptosis by repressing the PI3K/AKT survival pathway, we measured levels of PI3K and AKT by RT-PCR and Western blotting. As shown in Figures 9 to 11, emodin caused a decrease of PI3K and AKT in a dose-dependent manner

## *Emodin Upgraded PI3K-AKT Signaling Upstream of PTEN Gene*

The tumor suppressor PTEN was originally identified as a negative regulator of PI3K signaling, a main regulator of cell growth, metabolism, and survival. Yet this function of PTEN is extremely relevant for its tumor-suppressive ability, albeit the recent characterization of many PI3K-independent

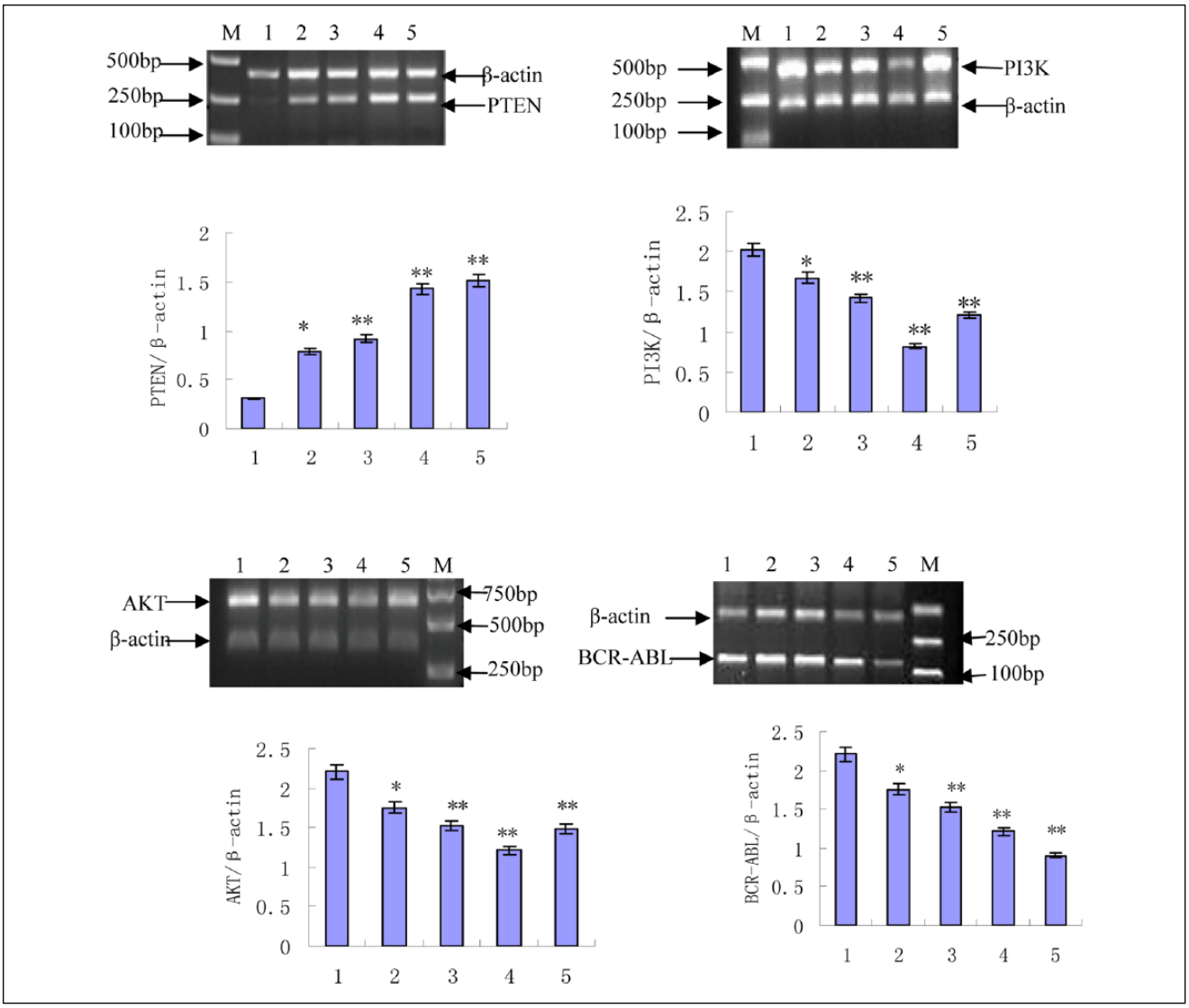


**Figure 10.** The mRNA expressions of PTEN, PI3K, AKT, and BCR-ABL in K562 cell from the emodin-treated group. RT-PCR analysis of the mRNA of PTEN, PI3K, AKT, and BCR-ABL obtained from nude mice tumor xenografts treated with emodin or HU. M: DNA marker; 1: negative control; 2: 25 mg/kg group; 3: 50 mg/kg group; 4: 100 mg/kg group; 5: positive control HU group. All RT-PCR were representative of 3 independent experiments (n = 3).

tumor-suppressive activities. The phosphatase and tensin homolog deletion on chromosome PTEN was originally discovered as a candidate tumor suppressor, mutated and lost in various cancers.[12,13] The major function of PTEN is the buffering of PI3K signaling. The loss and mutation of PTEN in various cancers lead to hyperactive PI3K signaling. PTEN is a main player in the regulation of PI3K signaling. As shown in Figures 9 to 11, our study showed emodin dose-dependently upgraded PTEN level in vitro and in vivo.

## Discussion

The search for new chemopreventive and antitumor agents that are more effective and less toxic has stimulated great interest in phytochemicals. Emodin, a natural anthraquinone derivative isolated from *Rheum palmatum* L, is one such compound. Results of the present study provided evidence to indicate that emodin exhibited antitumor activity in K562 cells in vitro and in vivo through apoptosis induction. The mechanism was via inactivating PTEN/PI3K-AKT and deleting BCR-ABL

Although emodin exhibited very potent cytotoxicity toward K562 cell line by MTT, it did not exhibit very potent cytotoxicity toward normal human embryonic kidney 293 cells (data not shown), suggesting its tumor-selectivegrowth inhibitory effect. The results from animal experiments showed that after 12 days of treatment with emodin, no significant variation in body weight was detected (data not

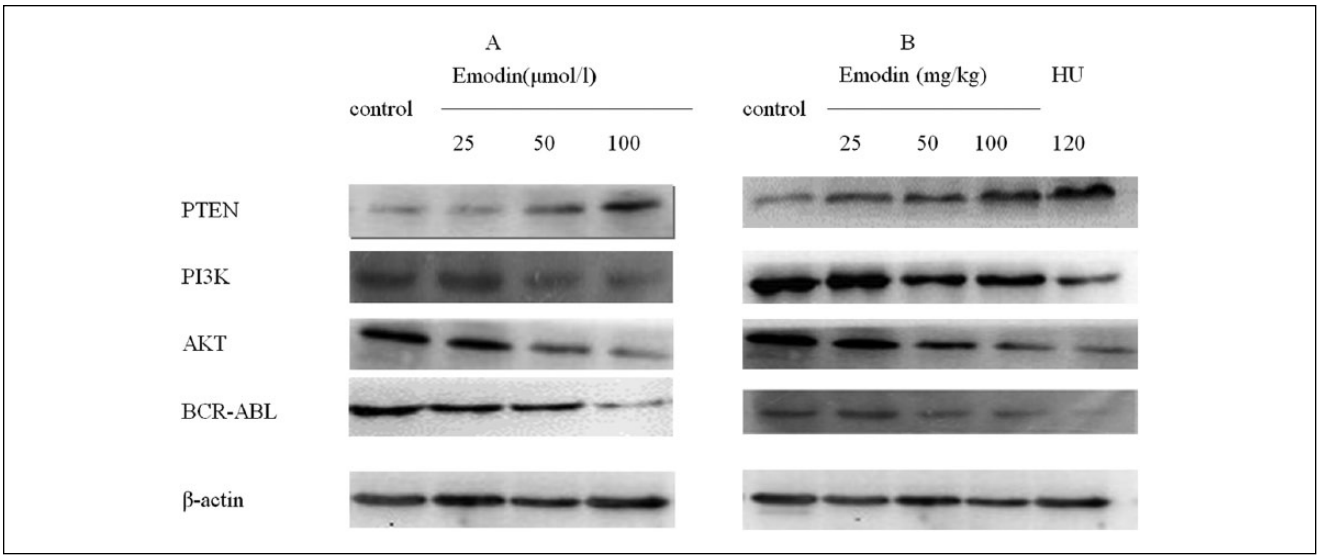


**Figure 11.** Involvement of PTEN, PI3K, AKT, and BCR-ABL proteins in emodin-induced apoptosis. (A) Western blotting analysis of PTEN, PI3K, AKT, and BCR-ABL proteins of K562 cells treated with the indicated concentration of emodin for 36 hours, respectively. (B) Western blotting analysis of PTEN, PI3K, AKT, and BCR-ABL of the protein extracts obtained from nude mice tumor xenograft treated with the indicated concentration of emodin or HU. All Western blots were representative of 3 independent experiments (n = 3).

shown), suggesting that emodin did not produce significant nontumor toxicity in tumor-bearing mice. But in the hydroxyurea treatment group, the weight of nude mice (data not shown) was significantly lower than in the negative control group, accompanied by the formation of cachexia. All these results show that emodin is a potentially powerful anticancer drug with low toxicity and very few side effects.

The poor prognostic outcome of CML is due to its resistance to current therapies, maintaining it as a leading cause of cancer-related death. Successful treatment with chemotherapeutic agents is largely dependent on their ability to trigger cell death in tumor cells. Therefore, novel inducers of apoptosis provide a new therapeutic approach for anticancer design. Several previous studies have demonstrated that emodin exerts antitumorigenic activity by inducing apoptosis in cancer cells,[14-19] and sensitizes prostate cancer cells and gallbladder cancer cells to chemotherapeutic agents.[20,21] Apoptosis is an important way to maintain cellular homeostasis between cell division and cell death.[22] Apoptosis is a form of programmed cell death that is characterized by a variety of morphological features, including changes in the plasma membrane such as loss of membrane asymmetry and attachment, cell shrinkage, chromatin condensation, and chromosomal DNA fragmentation, so induction of apoptosis in cancer cells is one of the useful strategies for anticancer drug development.[23] In this respect, many studies were performed for screening of apoptosis inducing compounds from plants.[24-26] In the present study, we found that emodin showed significant antiproliferative activity and induction of apoptosis in K562 cells. We demonstrated the inhibition of proliferation of K562 cell growth in vivo with a corresponding reduction the tumor volume and weight of xenografted tumor in nude nice with emodin treatment. Preliminarily, we tested the role of emodin in induction of apoptosis by observing cellular morphology such as nuclear condensation, fragmentation of genomic DNA, and Annexin-V binding. Consistent with other studies, our results showed that there was an induction of apoptosis in K562 cells with emodin treatment. Induction of apoptosis and/or cell proliferation inhibition is highly correlated with the activation of a variety of intracellular signaling pathways to arrest the cell cycle in the $G_1$, S, or $G_2$ phase. In malignant tumors, cell population in the $G_1$ phase appears less frequent (<70%) than in normal tissue (>90%). The damage that causes $G_1$-check point arrest is believed to be an irreversible process and the cells ultimately undergo apoptosis. Our data indicated that emodin caused the increase of cells in the $G_1$ phase in a dose-dependent manner with the decrease of cells in diploid regions ($G_2$ and S phases). Thus, it could be concluded that emodin had the ability to induce apoptosis in proliferating cells. However, the cells in diploid regions seemed to have accumulated at the $G_1$ phase before shifting to the sub-diploid region as the percentage of cells at the diploid $G_1$ region greatly increased with the decrease of cells in the S and $G_2$ phases.

The Philadelphia (Ph) chromosome, first identified by Nowell and Hungerford in 1960, is the cytogenetic hallmark of CML.[27] The Ph chromosome is a shortened chromosome 22 that is a by-product of a reciprocal chromosomal translocation between the long arms of chromosomes 9 and 22, t(9;22)(q34;q11).[28] A consequence of this chromosomal translocation is the replacement of the first exon of the

cellular ABL non-receptor tyrosine kinase gene with sequences from the cellular BCR (break point cluster) gene,[29] resulting in a chimeric BCR-ABL oncoprotein with highly dysregulated, constitutive tyrosine kinase activity.[30] Three major forms of the BCR-ABL oncogene have been reported based on the break point occurring in the BCR gene. The most commonly occurring form of BCR-ABL is a 210 kDa oncoprotein that is found in most cases of CML and 5% to 10% of adults with acute leukemia. The other 2 forms of BCR-ABL are 230 kDa and 185 kDa proteins that are associated with chronic neutrophilic leukemia and acute lymphocytic leukemia, respectively.[31] Various studies have established that the BCR-ABL 210 kDa protein is oncogenic and is essential for the pathogenesis of CML.

The PI3Ks are a family oflipid kinases that catalyze the phosphorylation of phosphoinositides at the 30-hydroxyl group. A critical product of this reaction is phosphatidylinositol-3,4,5-trisphosphate (PIP3), a vital second messenger, which recruits downstream signaling proteins including Akt and the PDK1.[32] PDK1 phosphorylates and activates AKT. The PI3K pathway is frequently upregulated in human tumors.[33]The activation of the PI3K pathway is relatively well understood and is known to be a multistep process involving the PI3K-dependent phosphorylation of phospholipids localized at the plasma membrane, and the subsequent membrane localization of PDK1 and Ser/Thr kinase AKT (also known as protein kinase B) via their pleckstrin homology (PH) domains. The activation of PI3K ultimately leads to AKT phosphorylation at Thr308 and Ser473. Activated AKT controls fundamental cellular processes such as cell survival by phosphorylating and inactivating several downstream pro-apoptotic target molecules. The fact that AKT overexpression is found in many human cancers, that active AKT promotes resistance to chemo- and radiotherapy, and that AKT activity is sufficient to block apoptosis induced by a number of death stimuli has resulted in intensive studies on the role of AKT as a mediator of the PI3K survival signal. Elevated levels of phosphorylated PI3K/AKT can protect cells from undergoing apoptosis and contribute to drug resistance.[34] Therefore, inhibition of the PI3K/AKT pathway by pharmacological or genetic approaches may improve the response of cancer cells to chemotherapy.[35]As mentioned above, the treatment of cells with emodin alone or in combination with other chemotherapeutic agents has been shown to effectively counteract tumor progression, although the emodin-mediated molecular mechanism responsible for this effect remains to be fully elucidated. Given the importance of the aforementioned pathway in the modulation of tumor progression, the aim of the present study was to examine in detail how emodin affects the PI3K/AKT signaling pathway, leading to a cell death that biochemically resembles the typical features of apoptosis. We propose a model that supports the therapeutic validity of emodin in the treatment of human malignancies and other pathological conditions, since the emodin-mediated regulation of components of the PI3K pathway upstream of AKT leads to an effective downregulation of AKT kinase activity.

PTEN/PI3K/AKT constitutes an important pathway regulating the signaling of multiple biological processes such as apoptosis, metabolism, cell proliferation, and cell growth. PTEN is a major lipid 3-phosphatase, which signals down the PI3 kinase/AKT pro-apoptotic pathway. Furthermore, PTEN is a protein phosphatase, with the ability to dephosphorylate both serine and threonine residues. The protein-phosphatase activity has also been shown to regulate various cell-survival pathways, such as the mitogen-activated kinase (MAPK) pathway. It is well established that PTEN's lipid-phosphatase activity, via the PI3K/AKT pathway, mediates growth suppression functions.[36] Our results demonstrated that emodin can trigger apoptosis throughupregulating the expression of PTEN.

In brief, our results provide new insights that emodin can trigger apoptosis through the inhibition of PI3K/AKT level, upregulating the expression of PTEN anddeleting BCR-ABL.

Thus, in our findings emodin remarkably showed potent effects on the inhibition of K562 cells growth by inducing apoptosis. These results suggest that emodin may be developed as a promising chemotherapeutic agent in chronic myelocytic leukemia therapy in the future. The data also strongly support the view of the PTEN/PI3K/AKT pathway as an important target for drug discovery.

## Authors' Note

All applicable international, national, and/or institutional guidelines for the care and use of animals were followed.

## Declaration of Conflicting Interests

The author(s) declared no potential conflicts of interest with respect to the research, authorship, and/or publication of this article.

## Funding

The author(s) disclosed receipt of the following financial support for the research, authorship, and/or publication of this article: This study was funded by the National Natural Science Foundation of China (No. 81171658) and Scientific Research Foundation of the Chongqing Heath Bureau (No. 2011-2-285).

## References

1. Steelman LS, Pohnert SC, Shelton JG, Franklin RA, Bertrand FE, McCubrey. JAK/STAT, Raf/MEK/ERK, PI3K/Akt and BCR-ABL in cell cycle progression and leukemogenesis. *Leukemia*. 2004;18:189-218.
2. Olsen BB, Bjørling-Poulsen M, Guerra B. Emodin negatively affects the phosphoinositide 3-kinase/AKT signalling pathway: a study on its mechanism of action. *Int J Biochem Cell Biol*. 2007;39:227-237.

3. Fresno Vara JA, Casado E, Castro J, Cejas P, Belda-Iniesta C, González-Barón M. PI3K/Akt signalling pathway and cancer. *Cancer Treat Rev*. 2004;30:193-204.
4. Pixu L, Hailing C, Roberts TM. Targeting the phosphoinositide 3-kinase pathway in cancer. *Nat Rev Drug Discov*. 2009;8: 627-644.
5. Razis E, Bobos M, Kotoula V, et al. Evaluation of the association of PIK3CA mutations and PTEN loss with efficacy of trastuzumab therapy in metastatic breast cancer. *Breast Cancer Res Treat*. 2011;128:447-456.
6. Shieh DE, Chen YY, Yen MH, Chiang LC, Lin CC. Emodin-induced apoptosis through p53-dependent pathway in human hepatoma cells, *Life Sci*. 2004;74:2279-2290.
7. Wang C, Wu X, Chen M, et al. Emodin induces apoptosis through caspase 3-dependent pathway in HK-2 cells. *Toxicology*. 2007;231:120-128.
8. Chang YC, Lai TY, Yu CS. Emodin induces apoptotic death in murine myelomonocytic leukemia WEHI-3 cells in vitro and enhances phagocytosis in leukemia mice in vivo. *Evid Based Complement Alternat Med*. 2011;2011:523596.
9. Huang FJ, Hsuuw YD, Chan WH. Characterization of apoptosis induced by emodin and related regulatory mechanisms in human neuroblastoma cells. *Int J Mol Sci*. 2013;14: 20139-20156.
10. Lin SY, Lai WW, Ho CC, et al. Emodin induces apoptosis of human tongue squamous cancer SCC-4 cells through reactive oxygen species and mitochondria-dependent pathways. *Anticancer Res*. 2009;29:327-335.
11. Das SK, Guha AK. Biosorption of hexavalent chromium by *Termitomyces clypeatus* biomass: kinetics and transmission electron microscopic study. *J Hazard Mater*. 2009;167:685-691.
12. Li DM, Sun H. TEP, encoded by a candidate tumor suppressor locus, is a novel protein tyrosine phosphatase regulated by transforming growth factor beta. *Cancer Res*. 1997;57:2124-2129.
13. Carracedo A1, Pandolfi PP. The PTEN-PI3K pathway: of feedbacks and cross-talks. *Oncogene*. 2008;27:5527-5541.
14. Lee HZ, Hsu SL, Liu MC, Wu CH. Effects and mechanisms of aloe-emodin on cell death in human lung squamous cell carcinoma. *Eur J Pharmacol*. 2001;431:287-295.
15. Yaoxian W, Hui Y, Yunyan Z, Yanqin L, Xin G, Xiaoke W. Emodin induces apoptosis of human cervical cancer hela cells via intrinsic mitochondrial and extrinsic death receptor pathway. *Cancer Cell Int*. 2013;13:71.
16. Mulakayala C, Banaganapalli B, Mulakayala N, Pulaganti M, Anuradha CM, Chitta SK. Design and evaluation of new chemotherapeutics of aloe-emodin (AE) against the deadly cancer disease: an in silico study. *J Chem Biol*. 2013;6:141-153.
17. Lin ML, Lu YC, Chung JG, et al. Aloe-emodin induces apoptosis of human nasopharyngeal carcinoma cells via caspase-8-mediated activation of the mitochondrial death pathway. *Cancer Lett*. 2010;291:46-58.
18. Yu CX, Zhang XQ, Kang LD, et al. Emodin induces apoptosis in human prostate cancer cell LNCaP. *Asian J Androl*. 2008;10:625-634.
19. Jia X, Yu F, Wang J, et al. Emodin suppresses pulmonary metastasis of breast cancer accompanied with decreased macrophage recruitment and M2 polarization in the lungs. *Breast Cancer Res Treat*. 2014;148:291-302.
20. Huang XZ, Wang J, Huang C, et al. Emodin enhances cytotoxicity of chemotherapeutic drugs in prostate cancer cells: the mechanisms involve ROS-mediated suppression of multidrug resistance and hypoxia inducible factor-1. *Cancer Biol Ther*. 2008;7:468-475.
21. Wang W, Sun YP, Huang XZ, et al. Emodin enhances sensitivity of gallbladder cancer cells to platinum drugs via glutathion depletion and MRP1 downregulation. *Biochem Pharmacol*. 2010;79:1134-1140.
22. Hengartner MO. The biochemistry of apoptosis. *Nature*. 2000;407:770-776.
23. Renehan AG, Booth C, Potten CS. What is apoptosis, and why is it important to clinicians? *BMJ*. 2001;322:1536-1538.
24. Higashi K, Takasawa R, Yoshimori A, Goh T, Tanuma S, Kuchitsu K. Identification of a novel gene family, paralogs of inhibitor of apoptosis proteins present in plants, fungi, and animals. *Apoptosis*. 2005;10:471-480.
25. Cho WC, Leung KN. In vitro and in vivo anti-tumor effects of *Astragalus membranaceus. Cancer Lett*. 2007;252:43-54.
26. Wei YP, Guo YF, Sun GY. Effect of marchantin C derivative F41 on apoptosis of human cervical cancer HeLa cells. *Chin J Pharmacol Toxicol*. 2013;27:346-351.
27. Nowell PC, Hungerford DA. A minute chromosome in human chronic granulocytic leukemia. *Science*. 1960;142:1497.
28. Nowell PC. The minute chromosome (Phl) in chronic granulocytic leukemia. *Blut*. 1962;8(8):65-66.
29. Muller AJ, Young JC, Pendergast AM, et al. BCR first exon sequences specifically activate the BCR/ABL tyrosine kinase oncogene of Philadelphia chromosome-positive human leukemias. *Mol Cell Biol*. 1991;11:1785-1792.
30. Bedi A, Zehnbauer BA, Barber JP, Sharkis SJ, Jones RJ. Inhibition of apoptosis by BCR-ABL in chronic myeloid leukemia. *Blood*. 1994;83:2038-2044.
31. Li S, Ilaria RL Jr, Million RP, Daley GQ, Van Etten RA. The P190, P210, and P230 forms of the BCR/ABL oncogene induce a similar chronic myeloid leukemia–like syndrome in mice but have different lymphoid leukemogenic activity. *J Exp Med*. 1999;189:1399-1412.
32. Macdougall LK, Domin J, Waterfield MD. A family of phosphoinositide 3-kinases in *Drosophila* identifies a new mediator of signal transduction. *Cur Biol*. 1996;5:1404-1415.
33. Bartholomeusz C, Gonzalez-Angulo AM. Targeting the PI3K signaling pathway in cancer therapy. *Expert Opin Ther Targets*. 2012;16:121-130.
34. Courtney KD, Corcoran RB, Engelman JA. The PI3K pathway as drug target in human cancer. *J Clin Oncol*. 2010;28: 1075-1083.
35. Yi YW, Kang HJ, Kim HJ, Hwang JS, Wang A, Bae I. Inhibition of constitutively activated phosphoinositide 3-kinase/AKT pathway enhances antitumor activity of chemotherapeutic agents in breast cancer susceptibility gene 1-defective breast cancer cells. *Mol Carcinog*. 2013;52:667-675.
36. Carnero A, Blanco-Aparicio C, Renner O, Link W, Leal JF. The PTEN/PI3K/AKT signalling pathway in cancer, therapeutic implications. *Curr Cancer Drug Targets*. 2008;8:187-198.